bioRxiv preprint first posted online Nov. 29, 2017; doi: http://dx.doi.org/10.1101/226993. The copyright holder for this preprint (which was not peer-reviewed) is the author/funder. All rights reserved. No reuse allowed without permission.

CRISPR-Cas12a target binding unleashes single-stranded DNase activity

Janice S. Chen[1]†, Enbo Ma[1]†, Lucas B. Harrington[1]†, Xinran Tian[2] and Jennifer A. Doudna[1-5]*

Affiliations:

[1]Department of Molecular and Cell Biology

[2]Department of Chemistry

[3]Innovative Genomics Institute

[4]Howard Hughes Medical Institute

University of California, Berkeley, Berkeley, California 94720, USA.

[5]Molecular Biophysics & Integrated Bioimaging Division, Lawrence Berkeley National Laboratory, Berkeley, CA 94720, USA.

*Correspondence to: doudna@berkeley.edu

†These authors contributed equally to this work.

bioRxiv preprint first posted online Nov. 29, 2017; doi: http://dx.doi.org/10.1101/226993. The copyright holder for this preprint (which was not peer-reviewed) is the author/funder. All rights reserved. No reuse allowed without permission.

Abstract: CRISPR-Cas12a (Cpf1) proteins are RNA-guided DNA targeting enzymes that bind and cut DNA as components of bacterial adaptive immune systems. Like CRISPR-Cas9, Cas12a can be used as a powerful genome editing tool based on its ability to induce genetic changes in cells at sites of double-stranded DNA (dsDNA) cuts. Here we show that RNA-guided DNA binding unleashes robust, non-specific single-stranded DNA (ssDNA) cleavage activity in Cas12a sufficient to completely degrade both linear and circular ssDNA molecules within minutes. This activity, catalyzed by the same active site responsible for site-specific dsDNA cutting, indiscriminately shreds ssDNA with rapid multiple-turnover cleavage kinetics. Activation of ssDNA cutting requires faithful recognition of a DNA target sequence matching the 20-nucleotide guide RNA sequence with specificity sufficient to distinguish between closely related viral serotypes. We find that target-dependent ssDNA degradation, not observed for CRISPR-Cas9 enzymes, is a fundamental property of type V CRISPR-Cas12 proteins, revealing a fascinating parallel with the RNA-triggered general RNase activity of the type VI CRISPR-Cas13 enzymes.

One Sentence Summary: Cas12a (Cpf1) and related type V CRISPR interference proteins possess non-specific, single-stranded DNase activity upon activation by guide RNA-dependent DNA binding.

bioRxiv preprint first posted online Nov. 29, 2017; doi: http://dx.doi.org/10.1101/226993. The copyright holder for this preprint (which was not peer-reviewed) is the author/funder. All rights reserved. No reuse allowed without permission.

Main Text:

CRISPR-Cas adaptive immunity in bacteria and archaea uses RNA-guided nucleases to target and degrade foreign nucleic acids (*1, 2*). The CRISPR-Cas9 family of proteins has been widely deployed for gene editing applications (*3, 4*) based on the precision of double-stranded DNA (dsDNA) cleavage induced by two catalytic domains, RuvC and HNH, at sequences complementary to a guide RNA sequence (*5, 6*). A second family of enzymes, CRISPR-Cas12a (Cpf1), uses a single RuvC catalytic domain for guide RNA-directed dsDNA cleavage (*7-12*) **(Fig. 1a)**. Distinct from Cas9, Cas12a enzymes recognize a T-rich protospacer adjacent motif (PAM) (*7*), catalyze their own guide RNA (crRNA) maturation (*13*) and generate a PAM-distal dsDNA break with staggered 5' and 3' ends (*7*), features that have attracted interest for gene editing applications (*14-16*). However, the substrate specificity and DNA cleavage mechanism of Cas12a are yet to be fully elucidated.

While investigating substrate requirements for Cas12a activation, we tested *Lachnospiraceae* bacterium ND2006 Cas12a (LbCas12a) for guide RNA-directed single-stranded DNA (ssDNA) cleavage, a capability of diverse CRISPR-Cas9 orthologs (*17, 18*). Purified LbCas12a or *Streptococcus pyogenes* Cas9 (SpCas9) proteins **(fig. S1)** were assembled with guide RNA sequences targeting a circular, single-stranded M13 DNA phage. In contrast to SpCas9, we were surprised to find that LbCas12a induced rapid and complete degradation of M13 by a cleavage mechanism that could not be explained by sequence-specific DNA cutting **(Fig. 1b)**. This ssDNA shredding activity, not observed using an LbCas12a protein containing inactivating mutations in the RuvC catalytic domain, raised the possibility that a target-bound LbCas12a could degrade any ssDNA, regardless of complementarity to the guide RNA. To test this idea, we assembled LbCas12a or SpCas9 with a different guide RNA and complementary ssDNA with no sequence homology to M13 phage genome sequence, and added M13 DNA to

bioRxiv preprint first posted online Nov. 29, 2017; doi: http://dx.doi.org/10.1101/226993. The copyright holder for this preprint (which was not peer-reviewed) is the author/funder. All rights reserved. No reuse allowed without permission.

the reaction. Remarkably, LbCas12a catalyzed M13 degradation only in the presence of this complementary ssDNA "activator", an activity not observed for SpCas9 **(Fig. 1c)**. These findings reveal that binding of LbCas12a to a guide-complementary ssDNA unleashes robust, non-specific ssDNA *trans*-cleavage activity.

We next investigated the requirements for LbCas12-catalyzed *trans*-cleavage activity. Using a fluorophore quencher (FQ)-labeled reporter assay (*19, 20*), we assembled LbCas12a with its crRNA and either a complementary ssDNA, dsDNA or single-stranded RNA (ssRNA), and introduced an unrelated ssDNA- or ssRNA-FQ reporter in *trans* **(fig. S2)**. Both the crRNA-complementary ssDNA or dsDNA (the activator) triggered LbCas12a to cleave the ssDNA-FQ reporter substrate **(fig. S2A)**. However, ssRNA was neither capable of activating *trans*-cleavage nor susceptible to degradation by LbCas12a **(fig. S2B)**, confirming that LbCas12a harbors a DNA-activated general DNase activity.

To determine how LbCas12a-catalyzed ssDNA cleavage activity relates to site-specific dsDNA cutting, we tested the length requirements of the target strand (TS) and non-target strand (NTS) for LbCas12a activation using radiolabeled oligonucleotides. Although TS cutting occurred irrespective of the NTS length **(figs. S3A-B)**, NTS cleavage occurred only when the TS contained at least 15 nucleotides (nt) of complementarity with the crRNA **(fig. S3C)**. This showed that TS recognition is a prerequisite for NTS cutting. To test whether LbCas12a remains active for non-specific ssDNA cleavage after sequence-specific binding and cleavage of a dsDNA substrate, we first cut a dsDNA plasmid with an LbCas12a-crRNA complex, and introduced an unrelated dsDNA or ssDNA to the reaction **(Fig. 2a)**. Whereas non-specific dsDNA substrate remained intact, the ssDNA was rapidly degraded in a RuvC-domain dependent manner **(Fig. 2a; figs. S4, S5)**. Together, these results show that RNA-guided DNA

bioRxiv preprint first posted online Nov. 29, 2017; doi: http://dx.doi.org/10.1101/226993. The copyright holder for this preprint (which was not peer-reviewed) is the author/funder. All rights reserved. No reuse allowed without permission.

binding activates LbCas12a for both site-specific dsDNA cutting and non-specific ssDNA *trans*-cleavage.

The rapid degradation of a *trans* substrate suggested that the kinetics of LbCas12a-catalyzed site-specific dsDNA (*cis*-) cleavage and non-specific ssDNA (*trans*-) cleavage are fundamentally different. Stoichiometric titration experiments showed that *cis*-cleavage is single-turnover (*21*) **(Fig. 2b)**, whereas *trans*-cleavage is multiple-turnover **(Fig. 2c)**. Using the FQ assay, we found that LbCas12a-crRNA bound to a ssDNA activator molecule catalyzed ssDNA trans-cleavage at a rate of ~250 turnovers per second and a catalytic efficiency (k_{cat}/K_m) of 5.1×10^8 s^{-1} M^{-1}. When bound to a dsDNA activator, LbCas12a-crRNA catalyzed ~1250 turnovers per second with a catalytic efficiency approaching the rate of diffusion (*22*) with a k_{cat}/K_m of 1.7×10^9 s^{-1} M^{-1} **(Fig. 2d; fig. S6)**. These differences suggest that the NTS of the dsDNA activator helps stabilize the Cas12a complex in an optimal conformation for *trans*-ssDNA cutting.

We next tested the specificity of *trans*-cleavage activation using either a ssDNA or dsDNA activator. We found that the PAM sequence required for dsDNA binding by CRISPR-Cas12a (*21*) is critical for catalytic activation by a crRNA-complementary dsDNA (*8, 23*), but not for a crRNA-complementary ssDNA **(Fig. 3a)**. Two base-pair (bp) mismatches introduced along the crRNA-complementary sequence of either a ssDNA or dsDNA activator molecule slowed the *trans*-cleavage rate of a ssDNA-FQ reporter by up to ~100 fold, depending on the mismatch position. For only the dsDNA activator, alterations to the PAM sequence or mismatches between the crRNA and PAM-adjacent "seed region" also had large inhibitory effects on *trans*-ssDNA cleavage activity **(Fig. 3b; fig. S7)**, similar to the mismatch tolerance pattern observed in Cas12a off-target studies (*24-26*). Together, these data are consistent with

bioRxiv preprint first posted online Nov. 29, 2017; doi: http://dx.doi.org/10.1101/226993. The copyright holder for this preprint (which was not peer-reviewed) is the author/funder. All rights reserved. No reuse allowed without permission.

PAM-mediated dsDNA target binding and the role of base pairing between the crRNA and the target strand to activate *trans*-ssDNA cutting.

We next explored whether LbCas12a-catalyzed *trans*-ssDNA cleavage can distinguish between two closely-related dsDNA viruses, human papillomavirus (HPV) serotypes 16 (HPV16) and 18 (HPV18) (*27*). Within the HPV16 and HPV18 genomes, we selected a 20 nt target sequence located next to a TTTA PAM that varied by only six base pairs between the two serotypes **(Fig. 3c)**. Plasmids containing a ~500 bp fragment of the HPV16 or HPV18 genome, including the target sequence, were incubated with the LbCas12a-crRNA complex targeting either the HPV16 or HPV18 fragment and a fluorescent ssDNA reporter. Robust LbCas12a-catalyzed ssDNA *trans*-cleavage occurred only in the presence of the cognate HPV target **(Fig. 3c; fig. S8)**, suggesting that dsDNA recognition specificity and *trans*-cleavage activity could in principle be extended to detect any dsDNA sequence.

We wondered if this *trans*-ssDNA cutting activity might be a property of Cas12a, and perhaps more evolutionarily distinct type V CRISPR effector proteins, considering that all type V effectors contain a single RuvC nuclease domain (*28, 29*). We therefore purified Cas12a orthologs from *Acidaminococcus sp.* (AsCas12a) and *Francisella novicida* (FnCas12a), as well as a Cas12b protein from *Alicyclobacillus acidoterrestris* (AaCas12b) to test for *cis*- and *trans*-ssDNA cleavage activity. With varying efficiencies, all of these homologs catalyzed non-specific ssDNase cleavage when assembled with crRNA and a complementary ssDNA activator **(Fig. 4a)**, suggesting that target-dependent activation of non-specific ssDNA cleavage is a fundamental feature of all type V CRISPR-Cas12-family proteins.

Together, these findings support a unifying mechanism of target interference that begins with the Cas12a-guide RNA complex binding to a complementary DNA sequence in a PAM-

bioRxiv preprint first posted online Nov. 29, 2017; doi: http://dx.doi.org/10.1101/226993. The copyright holder for this preprint (which was not peer-reviewed) is the author/funder. All rights reserved. No reuse allowed without permission.

dependent (dsDNA) or PAM-independent (ssDNA) manner **(Fig. 4b)**. Within a host bacterium, such enzyme activation could provide simultaneous protection from both dsDNA and ssDNA phages, and could also target ssDNA sequences that arise temporarily during phage replication or transcription (*30*). For genome editing applications, this newly identified activity may also degrade single-stranded oligonucleotide donors that are often used for homology directed repair (*31*), altering DNA repair outcomes. Finally, these results reveal unexpected functional convergence of target-dependent *trans*-cleavage activity between the DNA-targeting type V and RNA-targeting type VI CRISPR effector enzymes (*19, 32, 33*) and broaden the antiviral capabilities of CRISPR interference.

bioRxiv preprint first posted online Nov. 29, 2017; doi: http://dx.doi.org/10.1101/226993. The copyright holder for this preprint (which was not peer-reviewed) is the author/funder. All rights reserved. No reuse allowed without permission.

References:

1. R. Sorek, V. Kunin, P. Hugenholtz, CRISPR--a widespread system that provides acquired resistance against phages in bacteria and archaea. *Nat Rev Microbiol* **6**, 181-186 (2008).
2. K. S. Makarova *et al.*, An updated evolutionary classification of CRISPR-Cas systems. *Nat Rev Microbiol* **13**, 722-736 (2015).
3. J. A. Doudna, E. Charpentier, Genome editing. The new frontier of genome engineering with CRISPR-Cas9. *Science* **346**, 1258096 (2014).
4. R. Barrangou, P. Horvath, A decade of discovery: CRISPR functions and applications. *Nat Microbiol* **2**, 17092 (2017).
5. M. Jinek *et al.*, A programmable dual-RNA-guided DNA endonuclease in adaptive bacterial immunity. *Science* **337**, 816-821 (2012).
6. J. S. Chen, J. A. Doudna, The chemistry of Cas9 and its CRISPR colleagues. *Nat Rev Chem* **1**, (2017).
7. B. Zetsche *et al.*, Cpf1 is a single RNA-guided endonuclease of a class 2 CRISPR-Cas system. *Cell* **163**, 759-771 (2015).
8. D. C. Swarts, J. van der Oost, M. Jinek, Structural Basis for Guide RNA Processing and Seed-Dependent DNA Targeting by CRISPR-Cas12a. *Mol Cell* **66**, 221-233 e224 (2017).
9. D. Dong *et al.*, The crystal structure of Cpf1 in complex with CRISPR RNA. *Nature* **532**, 522-526 (2016).
10. P. Gao, H. Yang, K. R. Rajashankar, Z. Huang, D. J. Patel, Type V CRISPR-Cas Cpf1 endonuclease employs a unique mechanism for crRNA-mediated target DNA recognition. *Cell Res* **26**, 901-913 (2016).

bioRxiv preprint first posted online Nov. 29, 2017; doi: http://dx.doi.org/10.1101/226993. The copyright holder for this preprint (which was not peer-reviewed) is the author/funder. All rights reserved. No reuse allowed without permission.

11. S. Stella, P. Alcon, G. Montoya, Structure of the Cpf1 endonuclease R-loop complex after target DNA cleavage. *Nature* **546**, 559-563 (2017).

12. T. Yamano *et al.*, Crystal Structure of Cpf1 in Complex with Guide RNA and Target DNA. *Cell* **165**, 949-962 (2016).

13. I. Fonfara, H. Richter, M. Bratovic, A. Le Rhun, E. Charpentier, The CRISPR-associated DNA-cleaving enzyme Cpf1 also processes precursor CRISPR RNA. *Nature* **532**, 517-521 (2016).

14. B. Zetsche *et al.*, Multiplex gene editing by CRISPR-Cpf1 using a single crRNA array. *Nat Biotechnol* **35**, 31-34 (2017).

15. X. Tang *et al.*, A CRISPR-Cpf1 system for efficient genome editing and transcriptional repression in plants. *Nat Plants* **3**, 17018 (2017).

16. Y. E. Tak *et al.*, Inducible and multiplex gene regulation using CRISPR-Cpf1-based transcription factors. *Nat Methods*, (2017).

17. Y. Zhang, R. Rajan, H. S. Seifert, A. Mondragon, E. J. Sontheimer, DNase H Activity of Neisseria meningitidis Cas9. *Mol Cell* **60**, 242-255 (2015).

18. E. Ma, L. B. Harrington, M. R. O'Connell, K. Zhou, J. A. Doudna, Single-Stranded DNA Cleavage by Divergent CRISPR-Cas9 Enzymes. *Mol Cell* **60**, 398-407 (2015).

19. A. East-Seletsky *et al.*, Two distinct RNase activities of CRISPR-C2c2 enable guide-RNA processing and RNA detection. *Nature* **538**, 270-273 (2016).

20. J. S. Gootenberg *et al.*, Nucleic acid detection with CRISPR-Cas13a/C2c2. *Science* **356**, 438-442 (2017).

21. D. Singh *et al.*, Real-time observation of DNA target interrogation and product release by the RNA-guided endonuclease CRISPR Cpf1. *bioRxiv*, (2017).

bioRxiv preprint first posted online Nov. 29, 2017; doi: http://dx.doi.org/10.1101/226993. The copyright holder for this preprint (which was not peer-reviewed) is the author/funder. All rights reserved. No reuse allowed without permission.

22. R. A. Alberty, G. G. Hammes, Application of the Theory of Diffusion-Controlled Reactions to Enzyme Kinetics. *J Phys Chem-Us* **62**, 154-159 (1958).

23. S. H. Sternberg, S. Redding, M. Jinek, E. C. Greene, J. A. Doudna, DNA interrogation by the CRISPR RNA-guided endonuclease Cas9. *Nature* **507**, 62-67 (2014).

24. D. Kim *et al.*, Genome-wide analysis reveals specificities of Cpf1 endonucleases in human cells. *Nat Biotechnol* **34**, 863-868 (2016).

25. B. P. Kleinstiver *et al.*, Genome-wide specificities of CRISPR-Cas Cpf1 nucleases in human cells. *Nat Biotechnol* **34**, 869-874 (2016).

26. H. K. Kim *et al.*, In vivo high-throughput profiling of CRISPR-Cpf1 activity. *Nat Methods* **14**, 153-159 (2017).

27. C. B. Woodman, S. I. Collins, L. S. Young, The natural history of cervical HPV infection: unresolved issues. *Nat Rev Cancer* **7**, 11-22 (2007).

28. S. Shmakov *et al.*, Diversity and evolution of class 2 CRISPR-Cas systems. *Nat Rev Microbiol* **15**, 169-182 (2017).

29. E. V. Koonin, K. S. Makarova, F. Zhang, Diversity, classification and evolution of CRISPR-Cas systems. *Curr Opin Microbiol* **37**, 67-78 (2017).

30. P. Samai *et al.*, Co-transcriptional DNA and RNA Cleavage during Type III CRISPR-Cas Immunity. *Cell* **161**, 1164-1174 (2015).

31. C. D. Richardson, G. J. Ray, M. A. DeWitt, G. L. Curie, J. E. Corn, Enhancing homology-directed genome editing by catalytically active and inactive CRISPR-Cas9 using asymmetric donor DNA. *Nature Biotechnology* **34**, 339-+ (2016).

32. O. O. Abudayyeh *et al.*, C2c2 is a single-component programmable RNA-guided RNA-targeting CRISPR effector. *Science* **353**, aaf5573 (2016).

bioRxiv preprint first posted online Nov. 29, 2017; doi: http://dx.doi.org/10.1101/226993. The copyright holder for this preprint (which was not peer-reviewed) is the author/funder. All rights reserved. No reuse allowed without permission.

33. A. A. Smargon *et al.*, Cas13b Is a Type VI-B CRISPR-Associated RNA-Guided RNase Differentially Regulated by Accessory Proteins Csx27 and Csx28. *Mol Cell* **65**, 618-630 e617 (2017).

Acknowledgments: We thank O. Mavrothalassitis, D. Burstein, D. Lee and members of the Doudna laboratory for comments and discussions. This research was supported in part by the Allen Distinguished Investigator Program, through The Paul G. Allen Frontiers Group, and the National Science Foundation (MCB-1244557 to J.A.D.). J.S.C. and L.B.H. are supported by National Science Foundation Graduate Research Fellowships. J.A.D. is an Investigator of the Howard Hughes Medical Institute and executive director of the Innovative Genomics Institute at the University of California, Berkeley and the University of California, San Francisco. J.A.D. is a co-founder of Editas Medicine, Intellia Therapeutics, and Caribou Biosciences and a scientific adviser to Caribou, Intellia, eFFECTOR Therapeutics and Driver. The Regents of the University of California have patents pending for CRISPR technologies on which the authors are inventors.

bioRxiv preprint first posted online Nov. 29, 2017; doi: http://dx.doi.org/10.1101/226993. The copyright holder for this preprint (which was not peer-reviewed) is the author/funder. All rights reserved. No reuse allowed without permission.

Figures:

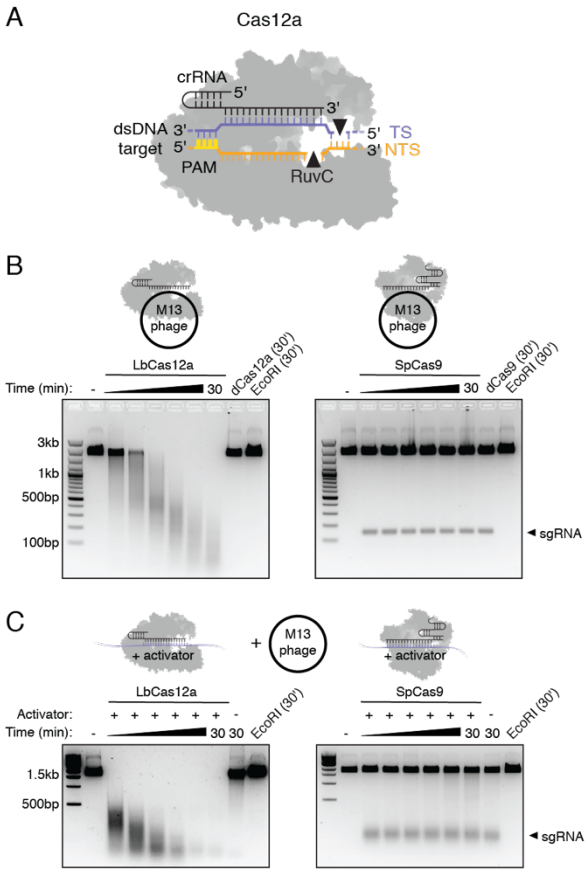


Fig. 1. **Cas12a target recognition activates non-specific single-stranded DNA cleavage.** (**A**) Cas12a-crRNA complex binds a dsDNA substrate and generates a 5' overhang staggered cut using a single RuvC nuclease. (**B, C**) Representative M13 ssDNA cleavage timecourses with purified LbCas12a (left) and SpCas9 (right) complexed with a (**B**) guide RNA complementary to M13 phage or (**C**) a guide RNA and complementary ssDNA activator with no sequence homology to M13 phage.

bioRxiv preprint first posted online Nov. 29, 2017; doi: http://dx.doi.org/10.1101/226993. The copyright holder for this preprint (which was not peer-reviewed) is the author/funder. All rights reserved. No reuse allowed without permission.

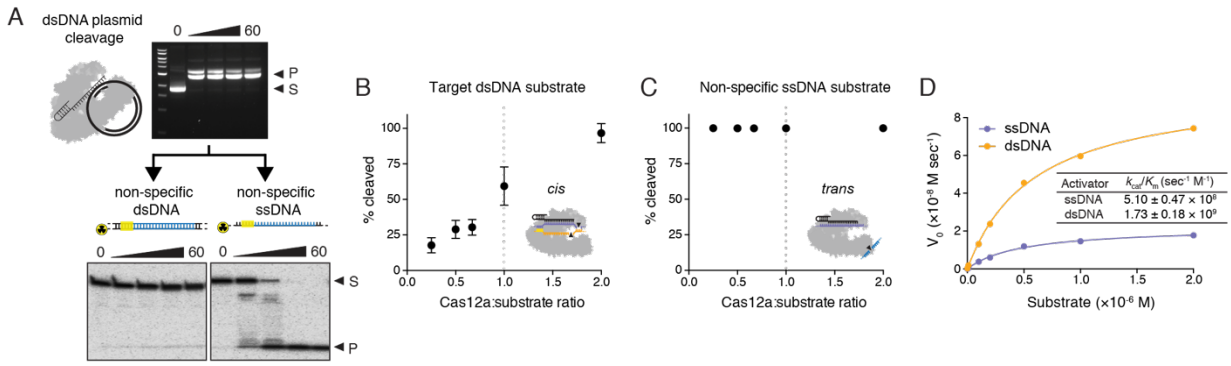


Fig. 2. Kinetics of Cas12a ssDNA *trans*-cleavage. (**A**) Sequence-specific plasmid DNA cleavage reactions by LbCas12a-crRNA (top) were introduce to a separate radiolabeled dsDNA or ssDNA substrate of unrelated sequence (bottom); timecourses represent minutes. (**B**) Target dsDNA or (**C**) non-specific ssDNA incubated with molar ratios of LbCas12a-crRNA as indicated. Each point represents the mean quantified percent cleavage after 30 minutes at 37°C, at which time the reaction was at completion. Error bars represent the mean ± s.d., where $n = 3$. (**D**) Representative Michaelis-Menten plot for LbCas12a-catalyzed ssDNA *trans*-cleavage using a dsDNA or ssDNA activator. Measured k_{cat}/K_m values report mean ± s.d., where $n = 3$.

bioRxiv preprint first posted online Nov. 29, 2017; doi: http://dx.doi.org/10.1101/226993. The copyright holder for this preprint (which was not peer-reviewed) is the author/funder. All rights reserved. No reuse allowed without permission.

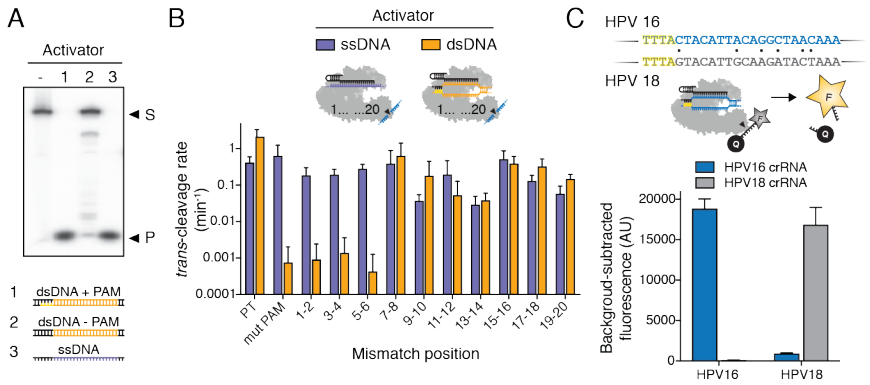


Fig. 3. Specificity of *trans*-cleavage activation. (**A**) LbCas12a-crRNA in the absence or presence of indicated activator, incubated with a radiolabeled non-specific ssDNA substrate (S) for 30 min at 37°C; products (P) resolved by denaturing PAGE. (**B**) Observed *trans*-cleavage rates for LbCas12a using a ssDNA or dsDNA activator with indicated mismatches; rates represent the average of three different targets measured in triplicate, and error bars represent mean ± s.d., where $n = 9$. (**C**) 20 base-pair target sequence with adjacent TTTA PAM (yellow) in related dsDNA human papillomavirus (HPV) serotypes 16 (HPV16) and 18 (HPV18) differs by six base pairs (black dots). Binding to a cognate HPV sequence activates LbCas12a trans-cleavage of the DNaseAlert substrate (see **Methods**) and generates a fluorescent signal. Background-subtracted maximum fluorescence values represent mean ± s.d., where $n = 3$.

bioRxiv preprint first posted online Nov. 29, 2017; doi: http://dx.doi.org/10.1101/226993. The copyright holder for this preprint (which was not peer-reviewed) is the author/funder. All rights reserved. No reuse allowed without permission.

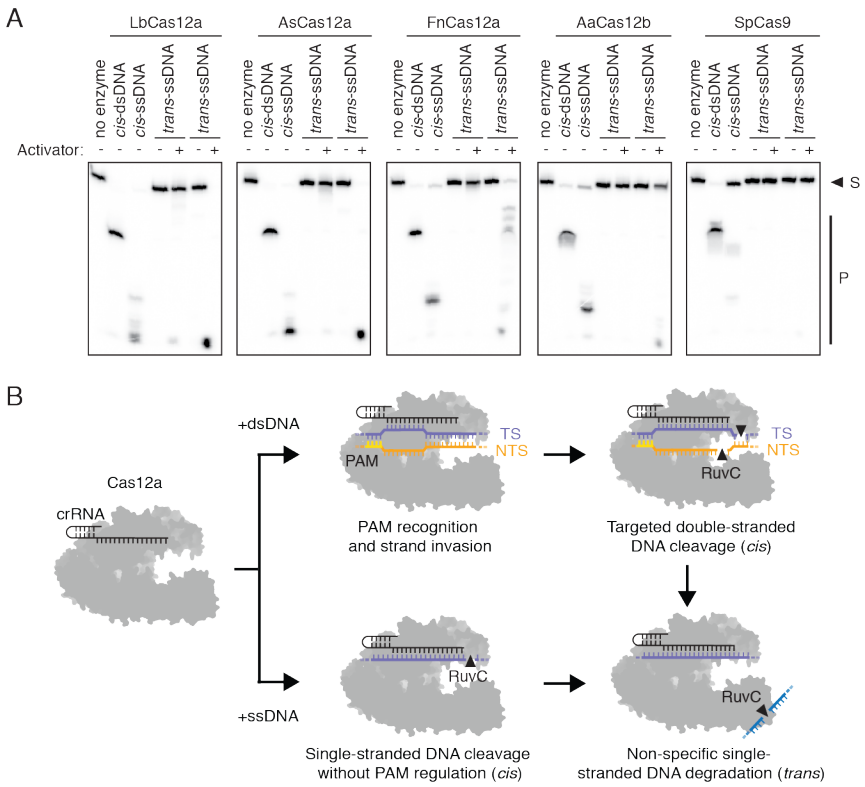


Fig. 4. Activator-dependent, non-specific ssDNA cleavage activity is conserved across type V CRISPR systems. (**A**) Radiolabeled *cis* (complementary) or *trans* (non-complementary) substrates were incubated with Cas12-crRNA or Cas9-sgRNA in the presence or absence of a ssDNA activator for 30 min at 37°C (or 47.5°C for AaCas12b); substrate (S) and nucleotide products (P) resolved by denaturing PAGE. (**B**) Model for PAM-dependent and PAM-independent activation of *cis* and *trans*-cleavage by Cas12a.

bioRxiv preprint first posted online Nov. 29, 2017; doi: http://dx.doi.org/10.1101/226993. The copyright holder for this preprint (which was not peer-reviewed) is the author/funder. All rights reserved. No reuse allowed without permission.

Materials and Methods

Protein expression and purification. SpCas9 and Cas12 proteins and mutants were cloned into a custom pET-based expression vector containing an N-terminal 10×His-tag, maltose-binding protein (MBP) and TEV protease cleavage site. Point mutations were introduced by around-the-horn PCR and verified by DNA sequencing. Proteins were purified as described (*1*), with the following modifications: *E. coli* BL21(DE3) containing SpCas9 or Cas12 expression plasmids were grown in Terrific Broth at 16°C for 14 hr. Cells were harvested and resuspended in Lysis Buffer (50 mM Tris-HCl, pH 7.5, 500 mM NaCl, 5% (v/v) glycerol, 1 mM TCEP, 0.5 mM PMSF and 0.25 mg/ml lysozyme), disrupted by sonication, and purified using Ni-NTA resin. After overnight TEV cleavage at 4°C, proteins were purified over an MBPTrap HP column connected to a HiTrap Heparin HP column for cation exchange chromatography. The final gel filtration step (Superdex 200) was carried out in elution buffer containing 20 mM Tris-HCl, pH 7.5, 200 mM NaCl (or 250 mM NaCl for AaCas12b), 5% (v/v) glycerol and 1 mM TCEP. All proteins tested in this study are shown in **fig. S1**.

Nucleic acid preparation. DNA substrates were synthesized commercially (IDT). For FQ-reporter assays, activator DNA duplexes were prepared by annealing 5-fold molar excess of the NTS to TS in 1× hybridization buffer (20 nM Tris-Cl, pH 7.5, 100 mM KCl, 5 mM $MgCl_2$), heating at 95°C and slow-cooling on the benchtop. HPV16 and HPV18 fragments were synthesized as gBlocks (IDT) and cloned into a custom pET-based vector via Gibson assembly. For radiolabeled cleavage assays, PAGE-purified DNA oligos were prepared as described.

sgRNA templates were PCR amplified from a pUC19 vector or overlapping primers containing a T7 promoter, 20 nucleotide target sequence and an sgRNA scaffold. The amplified PCR product served as the DNA template for *in vitro* transcription reactions, which were

bioRxiv preprint first posted online Nov. 29, 2017; doi: http://dx.doi.org/10.1101/226993. The copyright holder for this preprint (which was not peer-reviewed) is the author/funder. All rights reserved. No reuse allowed without permission.

performed as described (*1*). crRNAs were transcribed *in vitro* using a single-stranded DNA template containing a T7 promoter, repeat and spacer in the reverse complement orientation, which was annealed to T7 forward primer in 1× hybridization buffer. All DNA and RNA substrates are listed in **Table S1**.

DNA cleavage assays. Generally, Cas12a-mediated cleavage assays were carried out in Cleavage Buffer consisting of 20 mM HEPES (pH 7.5), 150 mM KCl, 10 mM $MgCl_2$, 1% glycerol and 0.5 mM DTT. For M13-targeting assays, 30 nM Cas12a was pre-assembled with either 36 nM of M13-targeting crRNA (*cis*) or with 36 nM of crRNA and 40 nM complementary ssDNA (activator) with no sequence homology to M13 (*trans*) at 37°C for 10 min. The reaction was initiated by adding 10 nM M13mp18 ssDNA (New England Biolabs) and incubated at 37°C for indicated timepoints. Reactions were quenched with DNA loading buffer (30% (v/v) glycerol, 0.25% (w/v) bromophenol blue, 0.25% (w/v) xylene cyanol) containing 15 mM EDTA and separated by 1.5% agarose gel pre-stained with SyberGold.

For radiolabeled cleavage assays, the substrates used were 5′-end-labeled with T4 PNK (NEB) in the presence of gamma ^{32}P-ATP. For dsDNA substrates, the non-target strand was first 5′-end-labeled and then annealed with excess corresponding target strand. The concentrations of Cas12a (or SpCas9), guide RNA and ^{32}P-labeled substrates used in the reaction were 30 nM, 36 nM and 1-3 nM, respectively. Reactions were incubated for 30 min (unless otherwise stated) at 37°C (or 47.5°C for the thermophilic AacCas12b) and quenched with formamide loading buffer (final concentration 45% formamide and 15 mM EDTA, with trace amount of xylene cyanol and bromophenol blue) for 3 min at 90°C. The substrates and products were resolved by 12% urea-denaturing PAGE gel and quantified with Amersham Typhoon (GE Healthcare).

bioRxiv preprint first posted online Nov. 29, 2017; doi: http://dx.doi.org/10.1101/226993. The copyright holder for this preprint (which was not peer-reviewed) is the author/funder. All rights reserved. No reuse allowed without permission.

For substrate turnover studies, the pre-assembled Cas12a-crRNA or Cas12a-crRNA-activator (target ssDNA or dsDNA) were incubated at 37°C for 10 min, and 30 nM of the pre-assembled RNP were used for each reaction with various substrate concentrations at 15, 30, 45, and 60 nM, respectively.

Fluorophore quencher (FQ)-labeled reporter assays. LbCas12a-crRNA complexes were pre-assembled by incubating 200 nM LbCpf1 with 250 nM crRNA and 4 nM activator (ssDNA, dsDNA or ssRNA) at 37°C for 30 min. The reaction was initiated by diluting LbCas12a complexes to a final concentration of 50 nM LbCas12a : 62.5 nM crRNA : 1 nM activator in a solution containing 1× Binding Buffer (20 mM Tris-HCl, pH 7.5, 100 mM KCl, 5 mM $MgCl_2$, 1 mM DTT, 5% glycerol, 50 μg ml^{-1} heparin) and 50 nM DNaseAlert substrate™ (IDT) or custom ssDNA/ssRNA FQ reporter substrates **(Table S1)**. Reactions were incubated in a fluorescence plate reader (Tecan Infinite Pro F200) for up to 120 minutes at 37°C with fluorescence measurements taken every 30 seconds (DNaseAlert substrate = λex: 535 nm; λem: 595 nm, custom ssDNA/ssRNA FQ substrates = λex: 485 nm; λem: 535 nm).

For *trans*-cleavage rate determination, background-corrected fluorescence values were calculated by subtracting fluorescence values obtained from reactions carried out in the absence of target plasmid. The resulting data were fit to a single exponential decay curve (GraphPad Software), according to the following equation: Fraction cleaved = $A \times (1 - \exp(-k \times t))$, where A is the amplitude of the curve, k is the first-order rate constant, and t is time.

For Michaelis-Menten analysis, LbCas12a-crRNA-activator (target ssDNA or dsDNA) complexes were prepared as described above, and reaction was initiated by diluting LbCas12a complexes to a final concentration of 5 nM LbCas12a : 6.25 nM crRNA : 0.1 nM activator (effective complex = 0.1 nM) in a solution containing 1× Binding Buffer and 0.001, 0.01, 0.1,

bioRxiv preprint first posted online Nov. 29, 2017; doi: http://dx.doi.org/10.1101/226993. The copyright holder for this preprint (which was not peer-reviewed) is the author/funder. All rights reserved. No reuse allowed without permission.

0.2, 0.5, 1 or 2 uM of DNaseAlert™ substrate (IDT). Reactions were incubated in a fluorescence plate reader for up to 30 minutes at 37°C with fluorescence measurements taken every 30 seconds (λex: 535 nm; λem: 595 nm). The initial velocity (V_0) was calculated by fitting to a linear regression and plotted against the substrate concentration to determine the Michaelis-Menten constants (GraphPad Software), according to the following equation: $Y = (V_{max} \times X)/(K_m + X)$, where X is the substrate concentration and Y is the enzyme velocity. The turnover number (k_{cat}) was determined by the following equation: $k_{cat} = V_{max}/E_t$, where E_t = 0.1 nM.

HPV detection assays were performed as above, with the following modifications: LbCas12a was pre-assembled with an HPV16 or HPV18-targeting crRNA and diluted in a solution containing 1× Binding Buffer, 50 nM DNaseAlert substrate™ (IDT) and 1, 10, 100, or 1000 nM of HPV16- or HPV18-containing plasmids. Reactions were incubated in a fluorescence plate reader for 60 minutes at 37°C with fluorescence measurements taken every 30 seconds (λex: 535 nm; λem: 595 nm).

bioRxiv preprint first posted online Nov. 29, 2017; doi: http://dx.doi.org/10.1101/226993. The copyright holder for this preprint (which was not peer-reviewed) is the author/funder. All rights reserved. No reuse allowed without permission.

Supplementary Figures S1-S8

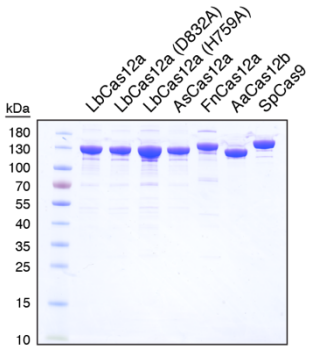


Fig. S1

Purification of Cas12 and Cas9 proteins. SDS-PAGE gel of all purified Cas12 and Cas9 proteins used in this study.

bioRxiv preprint first posted online Nov. 29, 2017; doi: http://dx.doi.org/10.1101/226993. The copyright holder for this preprint (which was not peer-reviewed) is the author/funder. All rights reserved. No reuse allowed without permission.

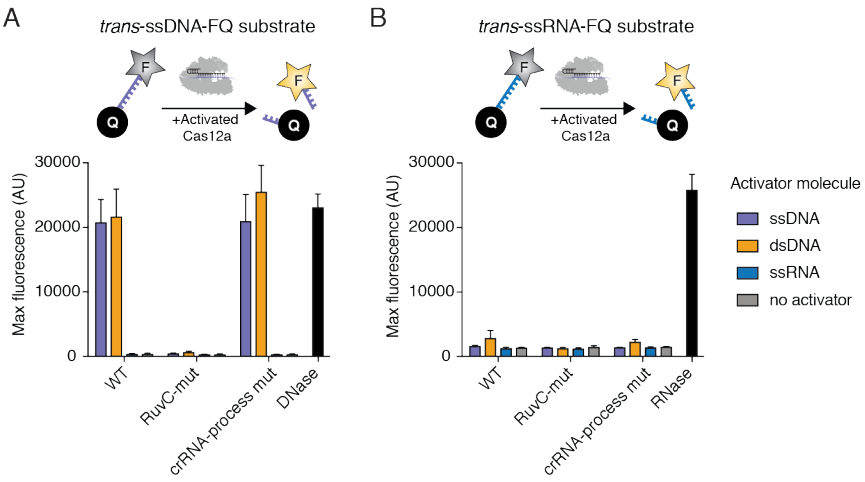


Fig. S2

LbCas12a is a DNA-activated general DNase. Quantification of maximum fluorescence signal generated after incubating LbCas12a-crRNA-activator with a custom (**A**) *trans*-ssDNA-FQ or (**B**) *trans*-ssRNA-FQ reporter for 1h at 37°C, with DNase I or RNase A controls where indicated. Error bars represent the mean ± s.d., where $n = 3$.

bioRxiv preprint first posted online Nov. 29, 2017; doi: http://dx.doi.org/10.1101/226993. The copyright holder for this preprint (which was not peer-reviewed) is the author/funder. All rights reserved. No reuse allowed without permission.

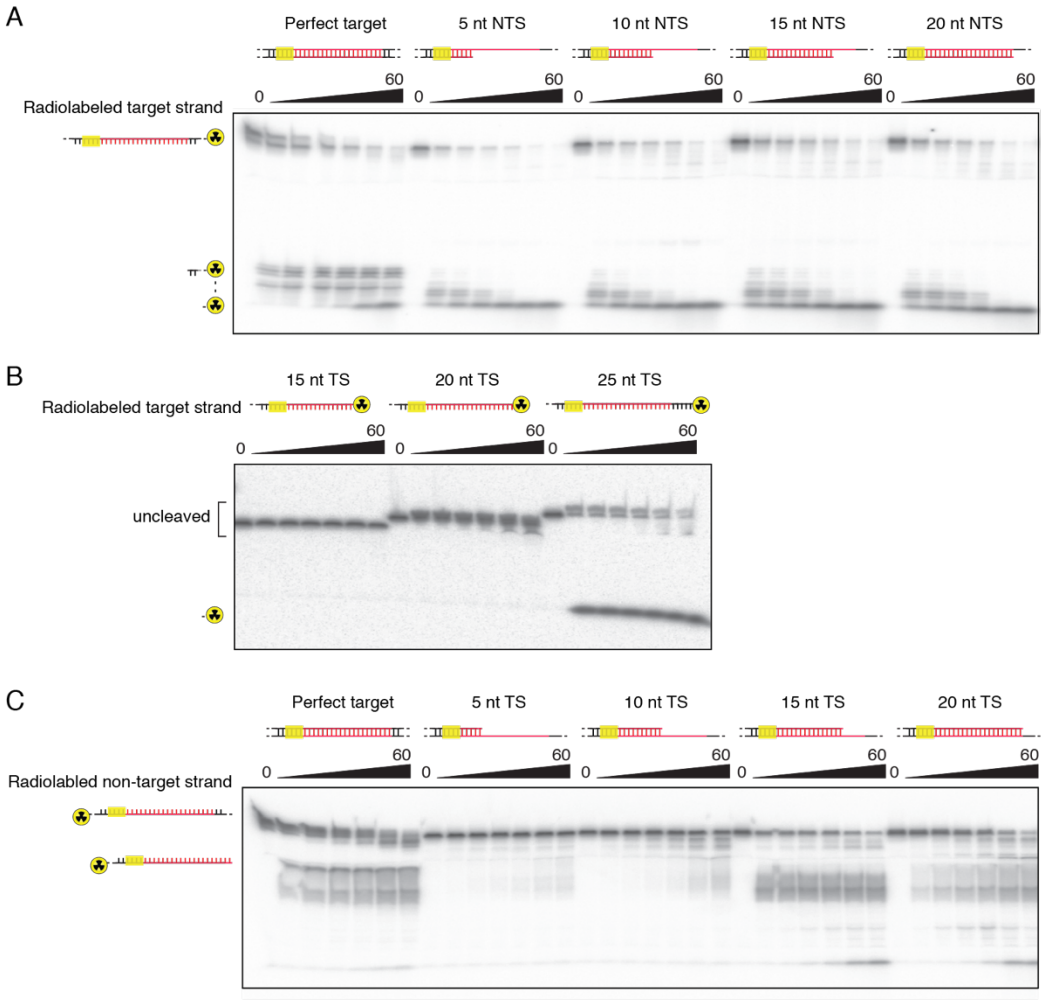


Fig. S3

Target strand recognition is a pre-requisite for single-stranded DNA cleavage. Cleavage timecourse assays using LbCas12a with (**A**) truncated target strand (TS) annealed to a radiolabeled non-target strand (NTS), (**B**) truncated and radiolabeled TS only, and (**C**) truncated NTS annealed to a radiolabeled TS. Timecourses represent minutes and cleavage products are resolved by denaturing PAGE.

bioRxiv preprint first posted online Nov. 29, 2017; doi: http://dx.doi.org/10.1101/226993. The copyright holder for this preprint (which was not peer-reviewed) is the author/funder. All rights reserved. No reuse allowed without permission.

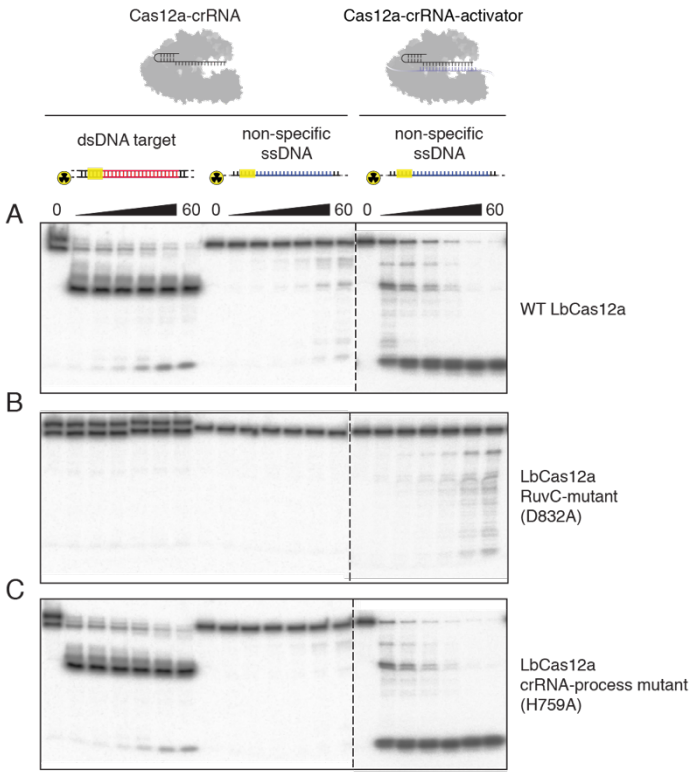


Fig. S4

The RuvC nuclease is responsible for activator-dependent, non-specific DNase activity.

Cleavage timecourse gel with radiolabeled target dsDNA and and non-specific ssDNA subsrates using (**A**) WT LbCas12a, (**B**) RuvC catalytic mutant (D832A) and (**C**) crRNA-processing mutant (H759A), with or without a ssDNA activator. Timecourses represent minutes and leavage products are resolved by denaturing PAGE.

bioRxiv preprint first posted online Nov. 29, 2017; doi: http://dx.doi.org/10.1101/226993. The copyright holder for this preprint (which was not peer-reviewed) is the author/funder. All rights reserved. No reuse allowed without permission.

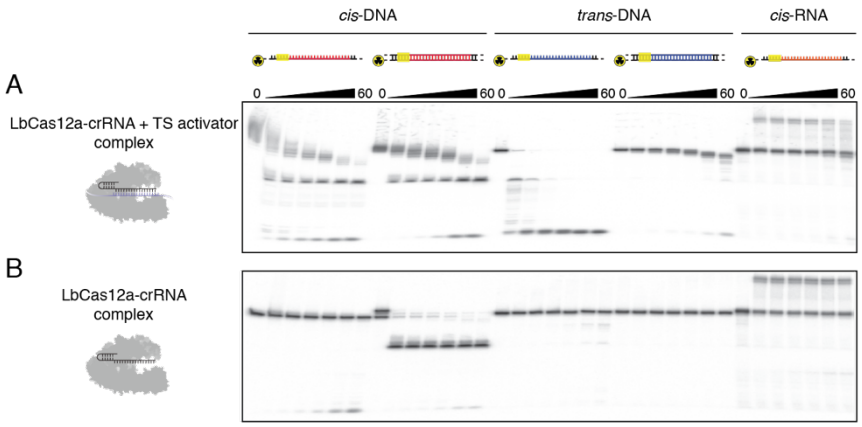
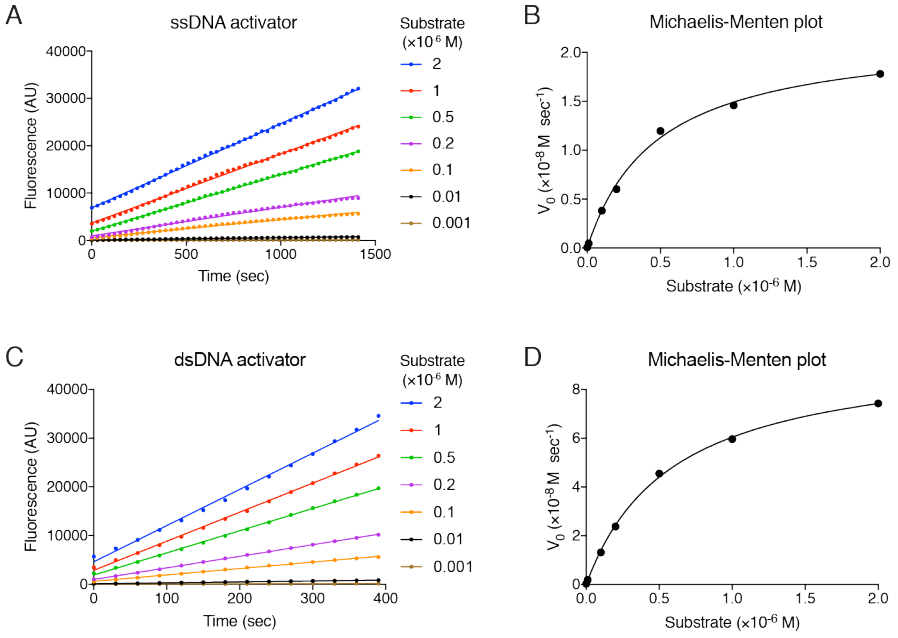


Fig. S5

LbCas12a *trans*-cleavage degrades complementary and non-specific ssDNA, but not ssRNA. Cleavage timecourse gels of LbCas12a-crRNA complexes using (**A**) a ssDNA activator or (**B**) no activator with indicated radiolabeled substrates where *cis* indicates a complementary target and *trans* indicates a non-complementary sequence. Timecourses represent minutes and cleavage products are resolved by denaturing PAGE.

bioRxiv preprint first posted online Nov. 29, 2017; doi: http://dx.doi.org/10.1101/226993. The copyright holder for this preprint (which was not peer-reviewed) is the author/funder. All rights reserved. No reuse allowed without permission.



E

Activator	k_{cat} (sec^{-1})	K_m (M^{-1})	k_{cat}/K_m ($sec^{-1}\ M^{-1}$)
ssDNA	$2.50 \pm 0.30 \times 10^{2}$	$4.94 \pm 0.16 \times 10^{-7}$	$5.10 \pm 0.47 \times 10^{8}$
dsDNA	$1.25 \pm 0.27 \times 10^{3}$	$7.25 \pm 1.74 \times 10^{-7}$	$1.73 \pm 0.18 \times 10^{9}$

Fig. S6

Michaelis-Menten analysis reveals robust *trans*-cleavage activity with a ssDNA and dsDNA activator. Representative plots of initial velocity versus time for a (**A**) ssDNA or (**C**) dsDNA activator, using 0.1 nM effective LbCas12a-crRNA-activator complex and increasing DNaseAlert substrate concentrations at 37°C. Michaelis-Menten fits for the corresponding (**B**) ssDNA or (**D**) dsDNA activator. (**E**) Calculated k_{cat}, K_m and k_{cat}/K_m values report the mean ± s.d., where $n = 3$.

bioRxiv preprint first posted online Nov. 29, 2017; doi: http://dx.doi.org/10.1101/226993. The copyright holder for this preprint (which was not peer-reviewed) is the author/funder. All rights reserved. No reuse allowed without permission.

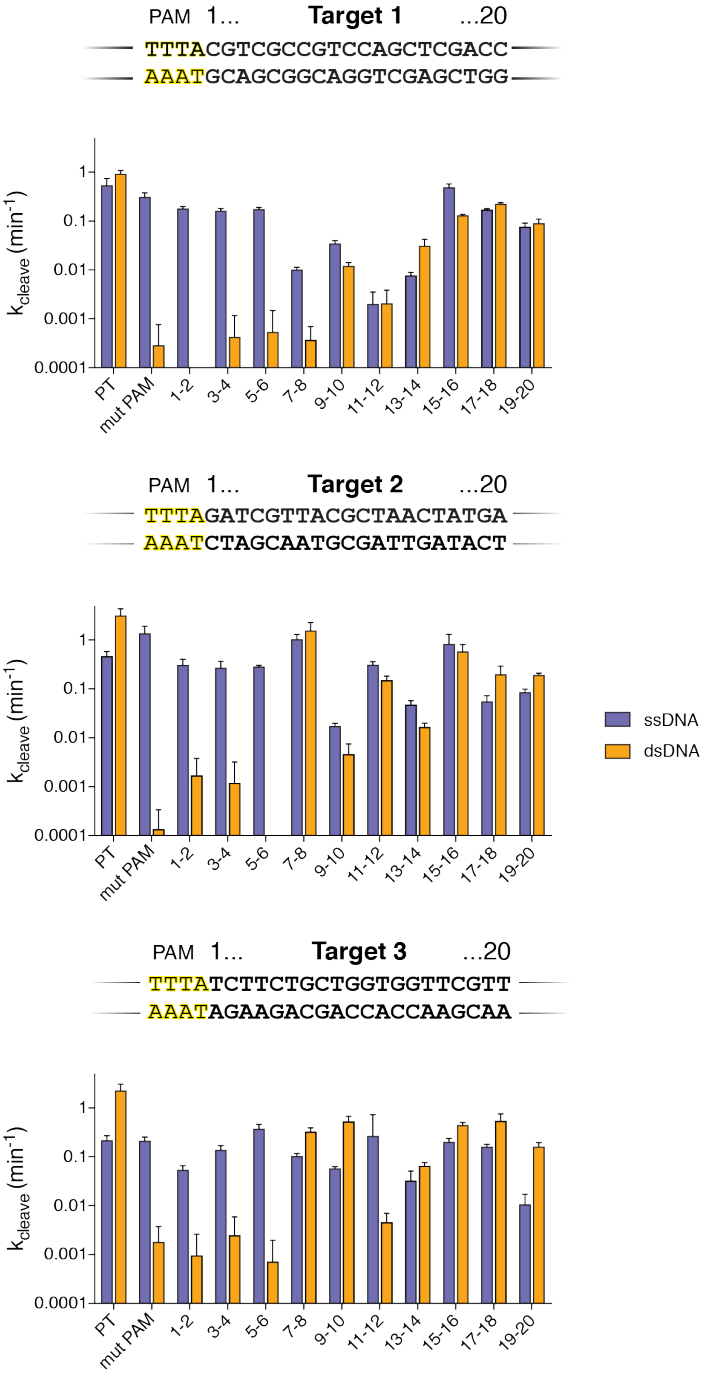


Fig. S7

The PAM sequence and PAM-proximal mismatches in a dsDNA activator provide specificity for *trans*-activation. Quantification of *trans*-cleavage kinetics using mismatched substrates for three distinct target sequences; error bars represent the mean ± s.d., where $n = 3$.

bioRxiv preprint first posted online Nov. 29, 2017; doi: http://dx.doi.org/10.1101/226993. The copyright holder for this preprint (which was not peer-reviewed) is the author/funder. All rights reserved. No reuse allowed without permission.

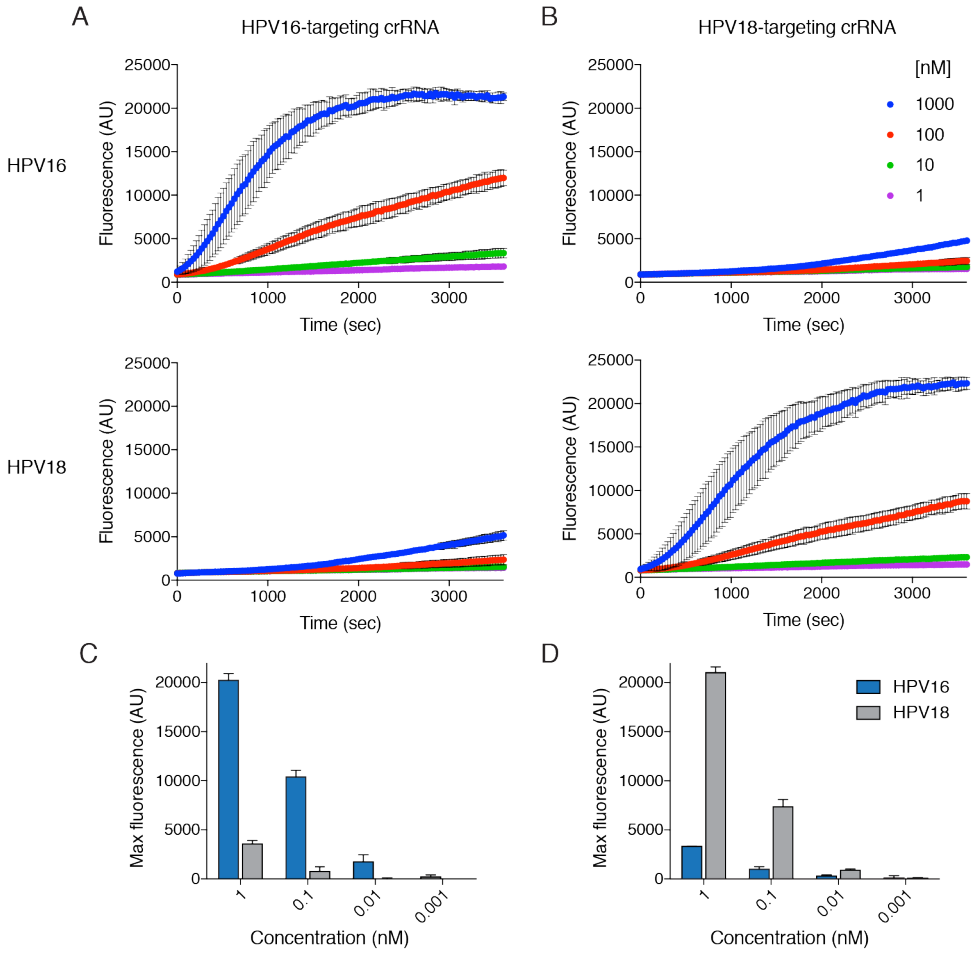


Fig. S8

Human papillomavirus (HPV) detection assay timecourse. Fluorescence timecourses with LbCas12a preassembled with a crRNA targeting (**A**) HPV16 or (**B**) HPV16 in the presence of a dsDNA plasmid containing an HPV16 (top row) or HPV18 (middle row) genomic fragment and DNaseAlert substrate, with fluorescence measurements taken every 30 seconds for 1h at 37°C. (**C**) Maximum fluorescence signal obtained from timecourses in (**A**) and (**B**). Error bars represent mean ± s.d., where $n = 3$.

bioRxiv preprint first posted online Nov. 29, 2017; doi: http://dx.doi.org/10.1101/226993. The copyright holder for this preprint (which was not peer-reviewed) is the author/funder. All rights reserved. No reuse allowed without permission.

Supplementary Table S1

RNA

LbCas12a crRNA - Target 1	UAAUUUCUACUAAGUGUAGAU**CGUCGCCGUCCAGCUCGACC**
LbCas12a crRNA - pUC19	UAAUUUCUACUAAGUGUAGAU**CAACGUCGUGACUGGGAAAACCCU**
LbCas12a crRNA - M13	UAAUUUCUACUAAGUGUAGAU**AACGAACCACCAGCAGAAGA**
LbCas12a crRNA - Target 2	UAAUUUCUACUAAGUGUAGAU**GAUCGUUACGCUAACUAUGA**
LbCas12a crRNA - Target 3	UAAUUUCUACUAAGUGUAGAU**CCUGGGUGUUCCACAGCUGA**
LbCas12a crRNA - HPV16	UAAUUUCUACUAAGUGUAGAU**CUACAUUACAGGCUAACAAA**
LbCas12a crRNA - HPV18	UAAUUUCUACUAAGUGUAGAU**GUACAUUGCAAGAUACUAAA**
AsCas12a crRNA - Target 2	UAAUUUCUACUCUUGUAGAU**GAUCGUUACGCUAACUAUGA**
FnCas12a crRNA - Target 2	UAAUUUCUACUGUUGUAGAU**GAUCGUUACGCUAACUAUGA**
AaCas12b crRNA - Target 2	GUCUAGAGGACAGAAUUUUUCAACGGGUGUGCCAAUGGCCACUUUCCAGGUGGCAAAGCCCGUUGAGCUUCUCAAAUCUGAGAAGUGGCAC**GAUCGUUACGCUAACUAUGA**
SpCas9 sgRNA - Target 1	**CGUCGCCGUCCAGCUCGACC**GUUUUAGAGCUAUGCUGUUUUGGAAACAAAACAGCAUAGCAAGUUAAAAUAAGGCUAGUCCGUUAUCAACUUGAAAAAGUGGCACCGAGUCGGUGC
SpCas9 sgRNA - M13	**AACGAACCACCAGCAGAAGA**GUUUUAGAGCUAUGCUGUUUUGGAAACAAAACAGCAUAGCAAGUUAAAAUAAGGCUAGUCCGUUAUCAACUUGAAAAAGUGGCACCGAGUCGGUGC
SpCas9 sgRNA - Target 2	**GAUCGUUACGCUAACUAUGA**GUUUUAGAGCUAUGCUGUUUUGGAAACAAAACAGCAUAGCAAGUUAAAAUAAGGCUAGUCCGUUAUCAACUUGAAAAAGUGGCACCGAGUCGGUGC
Target 1 ssRNA	GCCGGGGUGGUGCCCAUCCUGGUCGAGCUGGACGGCGACGUAAACGGCCACAAGC
Target 2 ssRNA	UAGCAUUCCACAGACAGCCCUCAUAGUUAGCGUAACGAUCUAAAGUUUUGUCGUC

Plasmids

M13mp18 ssDNA phage	https://benchling.com/s/seq-mnJjAqQ9tHfSPbKTNIPT
pUC19 dsDNA plasmid	https://benchling.com/s/seq-x4orD9lwDx2iHa6Ns3pR
HPV16-containing plasmid	https://benchling.com/s/seq-g0t5PySBcx4cwnz2h82w
HPV18-containing plasmid	https://benchling.com/s/seq-hv244BG5z20ON23SUZwq

DNA

non-specific NTS	AGCTTGTCTGCCATGGACATGCAGACTATACTGTTATTGTTGTACAGACCGAATTCCC
non-specific TS	GGGAATTCGGTCTGTACAACAATAACAGTATAGTCTGCATGTCCATGGCAGACAAGCT

Target 1_NTS	GCTTGTGGCCGTTTA**CGTCGCCGTCCAGCTCGACC**AGGATGGGCACCACCCCGGC
Target 1_TS	GCCGGGGTGGTGCCCATCCT**GGTCGAGCTGGACGGCGACG**TAAACGGCCACAAGC
Target 1_20-19_NTS	GCTTGTGGCCGTTTA**CGTCGCCGTCCAGCTCGA**GGAGGATGGGCACCACCCCGGC
Target 1_20-19_TS	GCCGGGGTGGTGCCCATCCTCC**TCGAGCTGGACGGCGACG**TAAACGGCCACAAGC
Target 1_18-17_NTS	GCTTGTGGCCGTTTA**CGTCGCCGTCCAGCTC**CTCCAGGATGGGCACCACCCCGGC
Target 1_18-17_TS	GCCGGGGTGGTGCCCATCCTGGAG**GAGCTGGACGGCGACG**TAAACGGCCACAAGC
Target 1_16-15_NTS	GCTTGTGGCCGTTTA**CGTCGCCGTCCAGC**AG**GACC**AGGATGGGCACCACCCCGGC
Target 1_16-15_TS	GCCGGGGTGGTGCCCATCCT**GGTC**CT**GCTGGACGGCGACG**TAAACGGCCACAAGC
Target 1_14-13_NTS	GCTTGTGGCCGTTTA**CGTCGCCGTCCA**CG**TCGACC**AGGATGGGCACCACCCCGGC
Target 1_14-13_TS	GCCGGGGTGGTGCCCATCCT**GGTCGA**CG**TGGACGGCGACG**TAAACGGCCACAAGC
Target 1_12-11_NTS	GCTTGTGGCCGTTTA**CGTCGCCGTC**GT**GCTCGACC**AGGATGGGCACCACCCCGGC
Target 1_12-11_TS	GCCGGGGTGGTGCCCATCCT**GGTCGAGC**AC**GACGGCGACG**TAAACGGCCACAAGC
Target 1_10-9_NTS	GCTTGTGGCCGTTTA**CGTCGCCG**AG**CAGCTCGACC**AGGATGGGCACCACCCCGGC
Target 1_10-9_TS	GCCGGGGTGGTGCCCATCCT**GGTCGAGCTG**CT**CGGCGACG**TAAACGGCCACAAGC
Target 1_8-7_NTS	GCTTGTGGCCGTTTA**CGTCGC**GC**TCCAGCTCGACC**AGGATGGGCACCACCCCGGC
Target 1_8-7_TS	GCCGGGGTGGTGCCCATCCT**GGTCGAGCTGGA**GC**GCGACG**TAAACGGCCACAAGC
Target 1_6-5_NTS	GCTTGTGGCCGTTTA**CGTC**CG**CGTCCAGCTCGACC**AGGATGGGCACCACCCCGGC
Target 1_6-5_TS	GCCGGGGTGGTGCCCATCCT**GGTCGAGCTGGACG**CG**GACG**TAAACGGCCACAAGC
Target 1_4-3_NTS	GCTTGTGGCCGTTTACG**AG**GCCGTCCAGCTCGACCAGGATGGGCACCACCCCGGC
Target 1_4-3_TS	GCCGGGGTGGTGCCCATCCT**GGTCGAGCTGGACGGC**CT**CG**TAAACGGCCACAAGC
Target 1_2-1_NTS	GCTTGTGGCCGTTTAGC**TCGCCGTCCAGCTCGACC**AGGATGGGCACCACCCCGGC
Target 1_2-1_TS	GCCGGGGTGGTGCCCATCCT**GGTCGAGCTGGACGGCGA**GC**TAAA**CGGCCACAAGC
Target 1_mut-PAM_NTS	GCTTGTGGCCGAGCA**CGTCGCCGTCCAGCTCGACC**AGGATGGGCACCACCCCGGC
Target 1_mut-PAM_TS	GCCGGGGTGGTGCCCATCCT**GGTCGAGCTGGACGGCGACG**TGCTCGGCCACAAGC

Target 1_5nt_TS	**CGACG**TAAACGGCCACAAGC
Target 1_10nt_TS	**GACGGCGACG**TAAACGGCCACAAGC
Target 1_15nt_TS	**AGCTGGACGGCGACG**TAAACGGCCACAAGC
Target 1_20nt_TS	**GGTCGAGCTGGACGGCGACG**TAAACGGCCACAAGC
Target 1_25nt_TS	A**TCCTGGTCGAGCTGGACGGCGACG**TAAACGGCCACAAGC

Target 1_5nt_NTS	GCTTGTGGCCGTTTA**CGTCG**
Target 1_10nt_NTS	GCTTGTGGCCGTTTA**CGTCGCCGTC**
Target 1_15nt_NTS	GCTTGTGGCCGTTTA**CGTCGCCGTCCAGCT**
Target 1_20nt_NTS	GCTTGTGGCCGTTTA**CGTCGCCGTCCAGCTCGACC**

bioRxiv preprint first posted online Nov. 29, 2017; doi: http://dx.doi.org/10.1101/226993. The copyright holder for this preprint (which was not peer-reviewed) is the author/funder. All rights reserved. No reuse allowed without permission.

Target 2_NTS	GACGACAAAACTTTAGATCGTTACGCTAACTATGAGGGCTGTCTGTGGAATGCTA
Target 2_TS	TAGCATTCCACAGACAGCCCTCATAGTTAGCGTAACGATCTAAAGTTTTGTCGTC
Target 2_20-19_NTS	GACGACAAAACTTTAGATCGTTACGCTAACTATCTGGGCTGTCTGTGGAATGCTA
Target 2_20-19_TS	TAGCATTCCACAGACAGCCCAGATAGTTAGCGTAACGATCTAAAGTTTTGTCGTC
Target 2_18-17_NTS	GACGACAAAACTTTAGATCGTTACGCTAACTTAGAGGGCTGTCTGTGGAATGCTA
Target 2_18-17_TS	TAGCATTCCACAGACAGCCCTCTAAGTTAGCGTAACGATCTAAAGTTTTGTCGTC
Target 2_16-15_NTS	GACGACAAAACTTTAGATCGTTACGCTAAGAATGAGGGCTGTCTGTGGAATGCTA
Target 2_16-15_TS	TAGCATTCCACAGACAGCCCTCATTCTTAGCGTAACGATCTAAAGTTTTGTCGTC
Target 2_14-13_NTS	GACGACAAAACTTTAGATCGTTACGCTTTCTATGAGGGCTGTCTGTGGAATGCTA
Target 2_14-13_TS	TAGCATTCCACAGACAGCCCTCATAGAAAGCGTAACGATCTAAAGTTTTGTCGTC
Target 2_12-11_NTS	GACGACAAAACTTTAGATCGTTACGGAAACTATGAGGGCTGTCTGTGGAATGCTA
Target 2_12-11_TS	TAGCATTCCACAGACAGCCCTCATAGTTTCCGTAACGATCTAAAGTTTTGTCGTC
Target 2_10-9_NTS	GACGACAAAACTTTAGATCGTTAGCCTAACTATGAGGGCTGTCTGTGGAATGCTA
Target 2_10-9_TS	TAGCATTCCACAGACAGCCCTCATAGTTAGGCTAACGATCTAAAGTTTTGTCGTC
Target 2_8-7_NTS	GACGACAAAACTTTAGATCGTATCGCTAACTATGAGGGCTGTCTGTGGAATGCTA
Target 2_8-7_TS	TAGCATTCCACAGACAGCCCTCATAGTTAGCGATACGATCTAAAGTTTTGTCGTC
Target 2_6-5_NTS	GACGACAAAACTTTAGATCCATACGCTAACTATGAGGGCTGTCTGTGGAATGCTA
Target 2_6-5_TS	TAGCATTCCACAGACAGCCCTCATAGTTAGCGTATGGATCTAAAGTTTTGTCGTC
Target 2_4-3_NTS	GACGACAAAACTTTAGAAGGTTACGCTAACTATGAGGGCTGTCTGTGGAATGCTA
Target 2_4-3_TS	TAGCATTCCACAGACAGCCCTCATAGTTAGCGTAACCTTCTAAAGTTTTGTCGTC
Target 2_2-1_NTS	GACGACAAAACTTTACTTCGTTACGCTAACTATGAGGGCTGTCTGTGGAATGCTA
Target 2_2-1_TS	TAGCATTCCACAGACAGCCCTCATAGTTAGCGTAACGAAGTAAAGTTTTGTCGTC
Target 2_mut-PAM_NTS	GACGACAAAACAGCAGATCGTTACGCTAACTATGAGGGCTGTCTGTGGAATGCTA
Target 2_mut-PAM_TS	TAGCATTCCACAGACAGCCCTCATAGTTAGCGTAACGATCTGCTGTTTTGTCGTC

Target 3_NTS	AGTTGTGTTAGTTTACCTGGGTGTTCCACAGCTGATAGTGATTGCCTTGAATAAA
Target 3_TS	TTTATTCAAGGCAATCACTATCAGCTGTGGAACACCCAGGTAAACTAACACAACT
Target 3_20-19_NTS	AGTTGTGTTAGTTTACCTGGGTGTTCCACAGCTCTTAGTGATTGCCTTGAATAAA
Target 3_20-19_TS	TTTATTCAAGGCAATCACTAAGAGCTGTGGAACACCCAGGTAAACTAACACAACT
Target 3_18-17_NTS	AGTTGTGTTAGTTTACCTGGGTGTTCCACAGGAGATAGTGATTGCCTTGAATAAA
Target 3_18-17_TS	TTTATTCAAGGCAATCACTATCTCCTGTGGAACACCCAGGTAAACTAACACAACT
Target 3_16-15_NTS	AGTTGTGTTAGTTTACCTGGGTGTTCCACTCCTGATAGTGATTGCCTTGAATAAA
Target 3_16-15_TS	TTTATTCAAGGCAATCACTATCAGGAGTGGAACACCCAGGTAAACTAACACAACT
Target 3_14-13_NTS	AGTTGTGTTAGTTTACCTGGGTGTTCCTGAGCTGATAGTGATTGCCTTGAATAAA
Target 3_14-13_TS	TTTATTCAAGGCAATCACTATCAGCTCAGGAACACCCAGGTAAACTAACACAACT
Target 3_12-11_NTS	AGTTGTGTTAGTTTACCTGGGTGTTGGACAGCTGATAGTGATTGCCTTGAATAAA
Target 3_12-11_TS	TTTATTCAAGGCAATCACTATCAGCTGTCCAACACCCAGGTAAACTAACACAACT
Target 3_10-9_NTS	AGTTGTGTTAGTTTACCTGGGTGAACCACAGCTGATAGTGATTGCCTTGAATAAA
Target 3_10-9_TS	TTTATTCAAGGCAATCACTATCAGCTGTGGTTCACCCAGGTAAACTAACACAACT
Target 3_8-7_NTS	AGTTGTGTTAGTTTACCTGGGACTTCCACAGCTGATAGTGATTGCCTTGAATAAA
Target 3_8-7_TS	TTTATTCAAGGCAATCACTATCAGCTGTGGAAGTCCCAGGTAAACTAACACAACT
Target 3_6-5_NTS	AGTTGTGTTAGTTTACCTGCCTGTTCCACAGCTGATAGTGATTGCCTTGAATAAA
Target 3_6-5_TS	TTTATTCAAGGCAATCACTATCAGCTGTGGAACAGGCAGGTAAACTAACACAACT
Target 3_4-3_NTS	AGTTGTGTTAGTTTACCACGGTGTTCCACAGCTGATAGTGATTGCCTTGAATAAA
Target 3_4-3_TS	TTTATTCAAGGCAATCACTATCAGCTGTGGAACACCGTGGTAAACTAACACAACT
Target 3_2-1_NTS	AGTTGTGTTAGTTTAGGTGGGTGTTCCACAGCTGATAGTGATTGCCTTGAATAAA
Target 3_2-1_TS	TTTATTCAAGGCAATCACTATCAGCTGTGGAACACCCACCTAAACTAACACAACT
Target 3_mut-PAM_NTS	AGTTGTGTTAGAGCACCTGGGTGTTCCACAGCTGATAGTGATTGCCTTGAATAAA
Target 3_mut-PAM_TS	TTTATTCAAGGCAATCACTATCAGCTGTGGAACACCCAGGTGCTCTAACACAACT

FQ substrates

ssDNA-FQ reporter	/56-FAM/TTATT/3IABkFQ/
ssRNA-FQ reporter	/56-FAM/rUrUrArUrU/3IABkFQ/
DNase-Alert substrate (IDT)	Proprietary

Table S1

Nucleic acids used in this study.

References:

1. M. Jinek *et al.*, Structures of Cas9 endonucleases reveal RNA-mediated conformational activation. *Science* **343**, 1247997 (2014).